A New SOLT Calibration Method for Leaky On-Wafer Measurements Using a 10-Term Error Model

Chen Liu, Aihua Wu, Chong Li, *Senior Member, IEEE*, and Nick Ridler, *Fellow, IEEE*

***Abstract*—We present a new short-open-load-thru (SOLT) calibration method for on-wafer S-parameter measurements. The new calibration method is based on a 10-term error model which is a simplified version of the 16-term error model. Compared with the latter, the former ignores all signal leakages except the ones between the probes. Experimental results show that this is valid for modern vector network analyzers. The advantage of using this 10-term error model is that the exact values of all error terms can be obtained by using the same calibration standards as the conventional SOLT method. This avoids not only the singularity problem with approximate methods, such as least squares, but also the usage of additional calibration standards. In this paper, we first demonstrate how the 10-term error model is developed, and then, the experimental verification of the theory is given. Finally, a practical application of the error model using a 10-dB attenuator from 140 to 220 GHz is presented. Compared with the conventional SOLT calibration method without crosstalk corrections, the new method shows approximately 1-dB improvement in the transmission coefficients of the attenuator at 220 GHz.**

***Index Terms*—Calibration, error model, millimeter-wave measurements, on-wafer measurements, scattering parameters.**

I. Introduction

FOR two-port on-wafer measurements, the probe tips are often very close to each other, causing probe-to-probe signal leakages or crosstalk as illustrated in Fig. 1. The crosstalk between probes affects measurement accuracy if it is not considered properly during system calibration and actual measurements. Fig. 2 shows the measured uncorrected raw data of $|S_{21}|$ for different impedance standards, i.e., open, short, and load on a commercial calibration substrate with a fixed probe separation of 150 μm in the frequency range from 140 to 220 GHz. These results show not only the crosstalk exists and could be as high as -15 dB, but also the crosstalk is dependent on the frequency and the devices under test (DUTs). The crosstalk is considered to consist of two parts: one is from the fringing effect which is related to the separation between the two probes. However, for on-wafer measurements at higher frequencies, e.g., 110 GHz and above, the probes need to be brought much closer together to reduce system losses, and thus, the fringing effect of the probes makes the probe-to-probe coupling stronger. This type of crosstalk contributes to the systematic error and can be corrected using system calibration; the other is related to the impedance of the DUT and it is difficult to correct using currently available system error models.

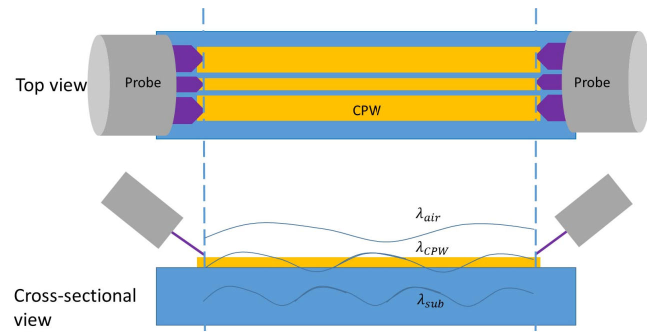

Fig. 1. Illustration of two-port on-wafer measurement and the probe-to-probe signal leakage due to fringing effects.

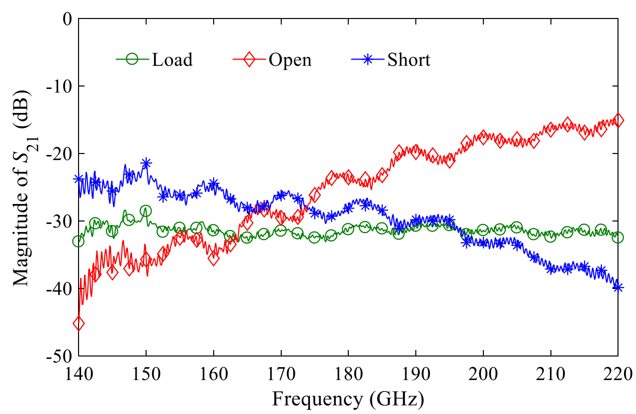

Fig. 2. Measured uncorrected raw data of $|S_{21}|$ for different impedance standards on a commercial calibration substrate with a fixed probe separation of 195 μm.

Manuscript received September 28, 2017; revised December 15, 2017 and February 8, 2018; accepted March 30, 2018. Date of publication June 14, 2018; date of current version August 6, 2018. This work was supported by the Research Project 14IND02 PlanarCal "Microwave Measurements for Planar Circuits and Components" through the European Metrology Program for Innovation and Research. The work of C. Liu and A. Wu was supported by the Hebei Semiconductor Research Institute. *(Corresponding author: Chong Li.)*

C. Liu and A. Wu are with the Department of Metrology and Maintenance, Hebei Semiconductor Research Institute, Shijiazhuang 050051, China (e-mail: liuchen0209@foxmail.com; aihua.wu@139.com).

C. Li was with the National Physical Laboratory, Teddington TW11 0LW, U.K. He is now with the Division of Electronics and Nanoscale Engineering, School of Engineering, University of Glasgow, Glasgow G12 8LT, U.K. (e-mail: chong.li@glasgow.ac.uk).

N. Ridler is with the Department of Engineering, Materials and Electrical Science, National Physical Laboratory, Teddington TW11 0LW, U.K. (e-mail: nick.ridler@npl.co.uk).

Color versions of one or more of the figures in this paper are available online at http://ieeexplore.ieee.org.

Digital Object Identifier 10.1109/TMTT.2018.2832052

0018-9480 © 2018 EU. Translations and content mining are permitted for academic research only. Personal use is also permitted, but republication/redistribution requires IEEE permission. See http://www.ieee.org/publications_standards/publications/rights/index.html for more information.

Most calibration methods used for coaxial, waveguide, or low-frequency on-wafer measurements, such as short-open-load-thru (SOLT), thru-reflect-line (TRL), and line-reflect-match (LRM), use either eight-term or 12-term error models that do not contain corrections for the crosstalk because it is either nonexistent or negligibly small [1]–[4]. The 16-term error model introduced by Speciale [5] in 1977 was the first to take into account the crosstalk between the vector network analyzer (VNA) measurement ports. Later, Butler *et al.* [6] and Heuermann and Schiek [7] demonstrated that the 16-term error model was able to correct crosstalk in a coaxial VNA system by deliberately adding an enclosed coaxial coupling network between the VNA and its test ports. It was Silvonen *et al.* [8], [9] who first implemented the 16-term error model for on-wafer measurements and developed the line-reflect-reflect-match calibration method. A simpler error model was then developed, based on the short-open-load-reciprocal (SOLR) method, as described in [10]. More recently, Williams *et al.* [11] investigated crosstalk and crosstalk corrections in a coplanar-waveguide (CPW) system using the 16-term error model and demonstrated that a number of factors, including the length of the access lines, transverse dimensions, the separation between the crosstalk standards, and the substrate configuration, etc., may play a role in correcting the crosstalk, and hence the achieved measurement accuracy.

There is no doubt that the probe-to-probe crosstalk should be corrected accurately during the system calibration and/or measurement. However, the fundamental problem with the 16-term error model is that there exist one or more singular values that make the exact values for all error terms not solvable if only four sets of two-port calibration standards are used. Numerical simulations performed in [12] show that at least five sets of two-port calibration standards including one or more nonsymmetrical standard pair (e.g., load short) are required to completely solve all the error terms in the 16-term error model. Using additional calibration standards is not desirable for on-wafer calibrations especially at millimeter-wave frequencies because it is difficult to design and fabricate the standards with sufficient accuracy.

In order not to use additional calibration standards, several methods have been developed to solve the error terms in the 16-term error model. One of the solutions is using the singular value decomposition (SVD) method to remove the singular values and obtain approximate values for the error terms [6], [13]. Other studies suggested that four or even three sets of two-port standards, as in the super-thru-short-delay approach, are possible under certain circumstances [5], [14]. In [8], four sets of calibration standards were also used, but the method was only suitable for reciprocal systems, or two-tier on-wafer calibrations.

In this paper, we propose a new and more general calibration method using a 10-term error model. The model is a simplified version of the 16-term error model, but ignores all leakages except the crosstalk between the test ports, or probes in this case. The main advantage of this model is that the singularity problem is avoided and all error terms in the model can be solved exactly without any assumptions or the need to introduce additional calibration standards. Only four sets of two-port standards that can be the same as the conventional SOLT standards, i.e., short–short, open–open, load–load, and a thru are required. The outline of this paper is as follows. The theory about the 10-term error model is first developed. Then, the experimental verification of the leakages is given. Finally, we demonstrate the implementation of the new error model for measurements of a 10-dB attenuator, and the results are compared with the conventional SOLT calibration as well as a numerical model.

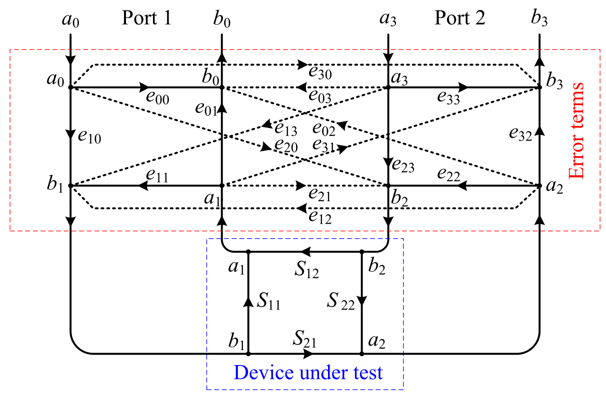

Fig. 3. Signal flowchart of the 16-term error model (Redrawn from [6]). The solid lines represent the actual signal transmission and reflection paths and the dotted lines represent the leakages or crosstalk.

II. Theory

A. 16-Term Error Model

Fig. 3 shows the signal flowchart of the 16-term error model for a two-port on-wafer S-parameter measurement system [6]. The solid lines represent the actual signal transmission and reflection paths, whereas the dotted lines represent the leakages or crosstalk between nodes. Compared with the conventional eight-term error model, the 16-term error model uses the same error network as a four-port network but adds eight signal leakage paths: between the test ports (in our case, these are the probe tips), e_{21} and e_{12}; between the test ports and the receivers, e_{13}, e_{31}, e_{02}, and e_{20}; and between the sources and the receivers inside the VNA, e_{30} and e_{03}. The error terms can be expressed in the form of a matrix [6] as shown in the following equation:

$$E = \begin{bmatrix} E_1 & E_2 \\ E_3 & E_4 \end{bmatrix} = \begin{bmatrix} e_{00} & e_{03} & e_{01} & e_{02} \\ e_{30} & e_{33} & e_{31} & e_{32} \\ e_{10} & e_{13} & e_{11} & e_{12} \\ e_{20} & e_{23} & e_{21} & e_{22} \end{bmatrix}. \tag{1}$$

Using S_a to represent the actual S-parameters of the DUT or the calibration standards and S_m to represent the measured S-parameters of the DUT or the calibration standards, we have the following:

$$S_m = E_1 + E_2 S_a (I - E_4 S_a)^{-1} E_3 \tag{2}$$

$$S_a = \{E_3 (S_m - E_1)^{-1} E_2 + E_4\}^{-1} \tag{3}$$

where I is the identity matrix. S_m and S_a can also be represented as

$$S_m = \begin{bmatrix} b_0/a_0 & b_0/a_3 \\ b_3/a_0 & b_3/a_3 \end{bmatrix} \tag{4}$$

$$S_a = \begin{bmatrix} a_1/b_1 & a_1/b_2 \\ a_2/b_1 & a_2/b_2 \end{bmatrix}. \tag{5}$$

Since the error terms in (3) are nonlinear and difficult to solve, one solution is to convert (1) to cascading T-parameters, as shown in the following equation, and then, (2) and (3) can be rewritten as (7) and (8), respectively,

$$T = \begin{bmatrix} T_1 & T_2 \\ T_3 & T_4 \end{bmatrix} = \begin{bmatrix} t_0 & t_1 & t_4 & t_5 \\ t_2 & t_3 & t_6 & t_7 \\ t_8 & t_9 & t_{12} & t_{13} \\ t_{10} & t_{11} & t_{14} & t_{15} \end{bmatrix} \tag{6}$$

$$S_a T_1 + T_2 - S_m T_3 S_a - S_m T_4 = 0 \tag{7}$$

$$S_a = (T_1 - S_m T_3)^{-1} (S_m T_4 - T_2). \tag{8}$$

At first glance, it appears that the four T terms in (7) can be solved using four equations formed with four sets of known calibration standards. Once the T terms are solved the actual S-parameters of a DUT can be derived using (8). However, this is not the case, because there are singularities in (2), and therefore (7), which make (7) and (8) not solvable with only four sets of equations. It has been demonstrated that at least five two-port calibration standards, including one nonsymmetrical pair (e.g., load short), can solve the equations accurately [12]. Alternatively, an approximation method, such as the SVD method, can be used to get close to (but not equal to) the exact values of the error terms [6], [13].

B. Error Term Matrix Transformation

It is necessary to include the matrix transformation between the E matrix and the T matrix before introducing the 10-term error model [14] shown in (9) and (10) at the bottom of this page, where

$$\Delta = t_{12}t_{15} - t_{13}t_{14} \tag{11}$$

$$\Delta_1 = t_4 t_{15} - t_5 t_{14} \tag{12}$$

$$\Delta_2 = t_5 t_{12} - t_4 t_{13} \tag{13}$$

$$\Delta_3 = t_6 t_{15} - t_7 t_{14} \tag{14}$$

$$\Delta_4 = t_7 t_{12} - t_6 t_{13} \tag{15}$$

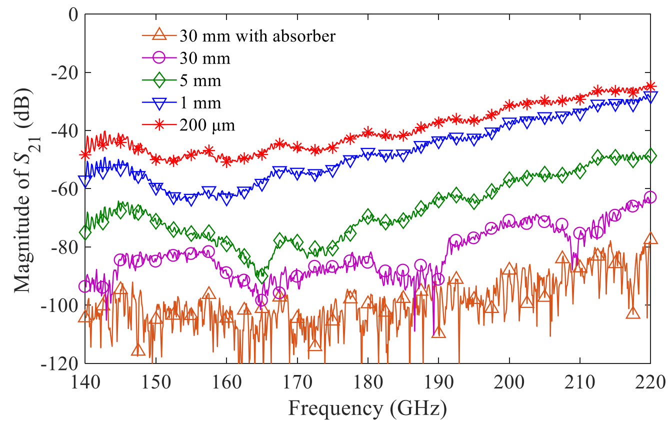

Fig. 4. Measured uncorrected raw data of $|S_{21}|$ for different separations between probes while probe tips are left in open air.

and

$$x = e_{10}e_{23} - e_{13}e_{20} \tag{16}$$

$$x_1 = e_{13}e_{21} - e_{23}e_{11} \tag{17}$$

$$x_2 = e_{20}e_{11} - e_{10}e_{21} \tag{18}$$

$$x_3 = e_{13}e_{22} - e_{23}e_{12} \tag{19}$$

$$x_4 = e_{20}e_{12} - e_{10}e_{22}. \tag{20}$$

As long as the T error terms are calculated, the E error terms can be derived using (9), and (11)–(15). On the contrary, the T error terms can be obtained from (10) and (16)–(20).

C. 10-Term Error Model

Assuming all the leakage or crosstalk terms from Fig. 3 are zero, the 16-term error model reduces to the conventional eight-term error model that is widely applied in TRL, LRM, and transmission type circuit-any circuit-unknown circuit [15], [16] calibration methods. However, for on-wafer measurement, the crosstalk error terms between probes, e_{21} and e_{12}, are necessary because the tips of both probes are exposed to the open environment and can be close to each other. The fringing effect from one probe couples energy to the other probe when they are within a close proximity. This is the case for components and transistors in monolithic millimeter-wave integrated circuits. Fig. 4 shows the measured coupling

$$\begin{aligned} E &= \begin{bmatrix} T_2 T_4^{-1} & T_1 - T_2 T_4^{-1} T_3 \\ T_4^{-1} & -T_4^{-1} T_3 \end{bmatrix} \\ &= \frac{1}{\Delta} \begin{bmatrix} \Delta_1 & \Delta_2 & \Delta t_0 - \Delta_1 t_8 - \Delta_2 t_{10} & \Delta t_1 - \Delta_1 t_9 - \Delta_2 t_{11} \\ \Delta_3 & \Delta_4 & \Delta t_2 - \Delta_3 t_8 - \Delta_4 t_{10} & \Delta t_3 - \Delta_3 t_9 - \Delta_4 t_{11} \\ t_{15} & -t_{13} & t_{10}t_{13} - t_8 t_{15} & t_{13}t_{11} - t_9 t_{15} \\ -t_{14} & t_{12} & t_8 t_{14} - t_{10}t_{12} & t_9 t_{14} - t_{11}t_{12} \end{bmatrix} \end{aligned} \tag{9}$$

$$\begin{aligned} T &= \begin{bmatrix} E_2 - E_1 E_3^{-1} E_4 & E_1 E_3^{-1} \\ -E_3^{-1} E_4 & E_3^{-1} \end{bmatrix} \\ &= \frac{1}{x} \begin{bmatrix} x e_{01} + x_1 e_{00} + x_2 e_{03} & x e_{02} + x_3 e_{00} + x_4 e_{03} & \cdots & \cdots & e_{00}e_{23} - e_{03}e_{20} & e_{03}e_{10} - e_{00}e_{13} \\ x e_{31} + x_1 e_{30} + x_2 e_{33} & x e_{32} + x_1 e_{30} + x_2 e_{33} & \cdots & \cdots & e_{30}e_{23} - e_{33}e_{20} & e_{33}e_{10} - e_{30}e_{13} \\ x_1 & x_3 & \cdots & \cdots & e_{23} & -e_{13} \\ x_2 & x_4 & \cdots & \cdots & -e_{20} & e_{10} \end{bmatrix} \end{aligned} \tag{10}$$

between two G-band (from 140 to 220 GHz) probes when they are placed in air and separated by various distances. The measured uncorrected raw data (i.e., the transmission coefficient S_{21}) is close to -20 dB at 220 GHz when the probes are separated by only 200 μm. The coupling will be higher when the probes are even closer and/or the frequency is higher. Therefore, it is necessary to remove, or calibrate out, the probe-to-probe crosstalk.

As shown in Fig. 3, error terms e_{30} and e_{03} are the leakage paths between the source and the receiver inside the VNA. For a modern network analyzer, the internal leakages are usually less than -60 dB (even at terahertz frequencies [17]) and so can be neglected. Other leakage terms, i.e., e_{20}, e_{02}, e_{31}, and e_{13}, have no direct physical paths between nodes but are the leakages from the VNA's ports to the reference planes, which are low-level noise and so can also be neglected [18]. Our experimental results also demonstrate the leakages from these terms are minimal. We will illustrate this point later.

In summary, based on the aforementioned analysis, we consider omitting all leakage terms except e_{21} and e_{12} in the 16-term error model. Thus, we have

$$e_{20} = e_{02} = e_{31} = e_{13} = e_{30} = e_{03} = 0 \tag{21}$$

so that only 10 error terms remain nonzero in the 16-term error model which now becomes a 10-term error model.

By substituting (21) into (10), the T matrix becomes

$$T = \begin{bmatrix} e_{01} - e_{00}e_{11}/e_{10} & -e_{00}e_{12}/e_{10} & e_{00}/e_{10} & 0 \\ -e_{21}e_{33}/e_{23} & e_{32} - e_{22}e_{33}/e_{23} & 0 & e_{33}/e_{23} \\ -e_{11}/e_{10} & -e_{12}/e_{10} & 1/e_{10} & 0 \\ -e_{21}/e_{23} & -e_{22}/e_{23} & 0 & 1/e_{23} \end{bmatrix}. \tag{22}$$

Thus, the 16 unknowns in (10) are reduced to 12 unknowns in (22). In the meantime, we can also obtain the following equations:

$$t_1 t_{12} = t_4 t_9 \tag{23}$$
$$t_2 t_{15} = t_7 t_{10}. \tag{24}$$

Although these two equations, i.e., (23) and (24) are not used for solving the error model, they provide useful supplementary information. For example, this information can be used to verify whether the solution to the error model is within the allowed range.

Now, if we use four sets of known two-port standards to perform the calibration, we will have a total of 18 equations, which are the 16 equations from (7) and the two equations from (23) and (24), to solve for the 12 unknowns. However, experiments have shown that sufficient accuracy is achieved by using only the 16 (linear) equations from (22) to solve for the 12 unknowns. If the additional two (nonlinear) equations in (23) and (24) are included, the accuracy of the solutions is not improved. In fact, the accuracy can be made worse by the need to use a more complicated nonlinear constrained optimization algorithm to solve for these additional terms.

To solve the overdetermined 12 unknowns for the T matrix, the homogeneous equations can be transformed to nonhomogeneous equations by normalizing the 12 unknown terms to any one term whose value is not zero. It is preferable to do this with t_{12} or t_{15}. Once this is done, the remaining 11 terms are calculated as a function of the normalized term. The detailed calculation can be found in textbooks (or refer to [6] and [14]) and so will not be repeated here. However, we carried out a simulation test on singularities using our in-house developed MATLAB code and so we were able to confirm that there is no singular solution for the E error terms.

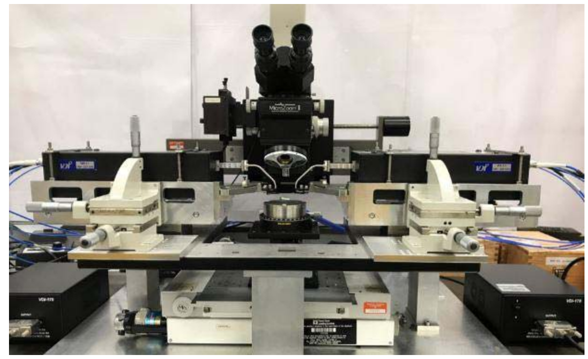

(a)

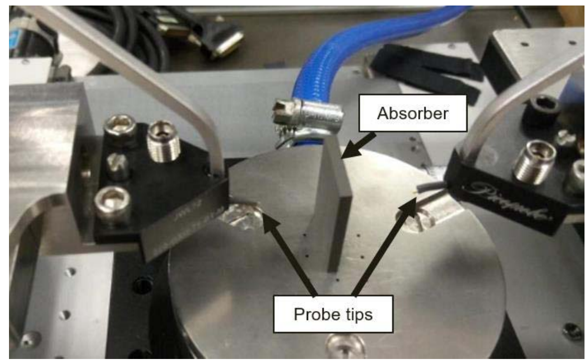

(b)

Fig. 5. (a) Photograph of the G-band (from 140 to 220 GHz) on-wafer S-parameter measurement setup. (b) Close-up showing a microwave absorber placed between the two lifted probes used to obtain some of the data shown in Fig. 4.

III. Implementation and Results

A. Verification of Leakages

In Section II-C, we described how the 10-term error model was derived from the 16-term error model by assuming that all leakage terms, apart from the probe-to-probe crosstalk, were neglected, without providing any evidence for the validity of this assumption. We now show experimentally that the assumption is valid. Because all leakage terms, except e_{21} and e_{12}, are independent of the separation between the two probes, we can, therefore, measure the leakages when the two probes are completely isolated; in other words, when e_{21} and e_{12} are equal to zero.

Fig. 5(a) shows the G-band (from 140 to 220 GHz) on-wafer S-parameter measurement setup, including a manual probe station, at the National Physical Laboratory, Teddington, U.K. Two probes from GGB Industries, Inc., are used in the setup. The system configuration is shown in Table I. During the leakage verification measurement, the two probes were

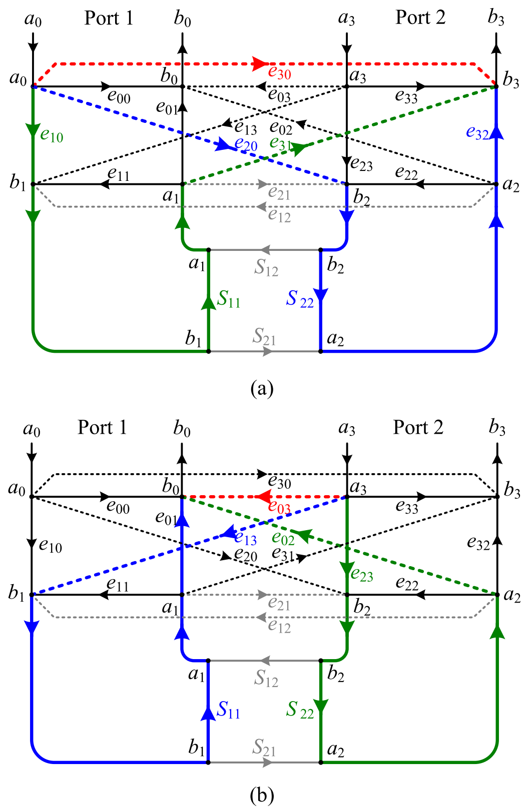

Fig. 6. (a) Forward signal flowchart of a two-port on-wafer network when two probes are "completely" isolated. (b) Reverse signal flowchart of a two-port on-wafer network when two probes are "completely" isolated.

TABLE I
SYSTEM CONFIGURATION

System Configuration	Model & Manufacturer / Parameters
VNA	PNA-X N5247A, Keysight
Frequency Extenders	WR5.1, VDI
Probe station	Customized Cascade (manual)
Probes	220-GSG-75-BT-M, GGB
No. of frequency points	801
IF bandwidth	100 Hz

lifted up in the air above the chuck by approximately 20 mm. Uncorrected raw transmission coefficients S_{21} were measured as the separation between the two probes was increased. The measurement results, plotted in Fig. 4, show that the transmission coefficients decrease as the separation distance between the probes increases, and reach −80 dB when the two probes are separated by 30 mm and −100 dB when a microwave absorber (Cascade PN 116-344) is inserted between the probes, as shown in Fig. 5(b). In this case, the two probes are completely isolated and there is no probe-to-probe coupling. In this situation, the transmission coefficients represent all signal leakages apart from e_{21} and e_{12}. If we now redraw the signal flowchart shown in Fig. 3 by separating the forward and the reverse paths, we mimic how a VNA measures the S-parameters of a two-port network. This is shown in Fig. 6. Taking the forward transmission path as an example, one can

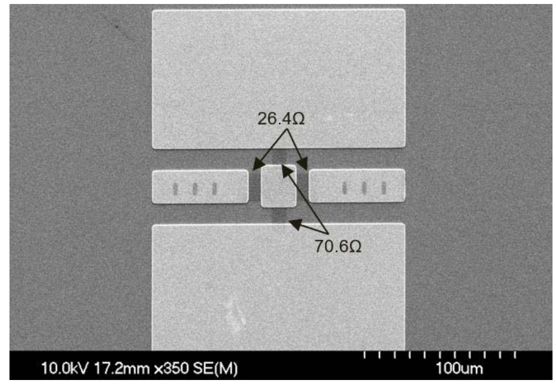

Fig. 7. SEM image of the attenuator. The attenuator was fabricated on a 4-in semi-insulating GaAs substrate using a standard photolithography method.

notice that the signal received at b_3 consists of three paths, which are as follows:

1) e_{30}, a direct path from a_0 to b_3, marked in red;
2) e_{20}—S_{22}—e_{32}, marked in blue;
3) e_{10}—S_{11}—e_{31}, marked in green.

As the transmission coefficients are below −80 dB, we can conclude that each individual path is also below −80 dB which is considered to be negligible. This simple experiment proves that our previous assumption of zero signal leakages, apart from e_{21} and e_{12}, is valid. In Section III-B, we demonstrate the implementation of the 10-term error model with the conventional SOLT standards for a G-band on-wafer system.

B. Implementation of the Error Model

A series of two-port standards including open–open pairs, short–short pairs, load–load pairs, and thrus were fabricated on a semi-insulating GaAs substrate using a standard photolithography technology. A 400-nm layer of gold was deposited for the conductors and a thin layer of nickel–chrome alloy was used for the resistors. The substrate was then thinned down to 100 μm after all circuits were made. To evaluate the calibration method, a 10-dB attenuator was designed with the aid of numerical software—Computer Simulation Technology (CST) Microwave Studio—and fabricated on the same substrate. The simulation uses wave ports, and is designed to determine the actual attenuator's response to a pure CPW mode that we hope to measure. Fig. 7 shows a scanning electron microscope (SEM) image of the attenuator. All aforementioned components have the same edge-to-edge distance (i.e., 160 μm) in order to keep the crosstalk constant during calibration and measurement. We defined the offset of the standards with reference to [19]. We used the setup shown in Fig. 5(a) to obtain uncorrected raw data for the SOLT calibration standards and the attenuator and then post-processed the data by implementing the conventional 12-term error model (assuming no probe-to-probe crosstalk) and the proposed 10-term error model.

Fig. 8 shows the comparisons of the transmission coefficients of the attenuator, corrected using the two error models, with the simulated data (using CST). In addition, we also plot the results corrected using the conventional SOLT

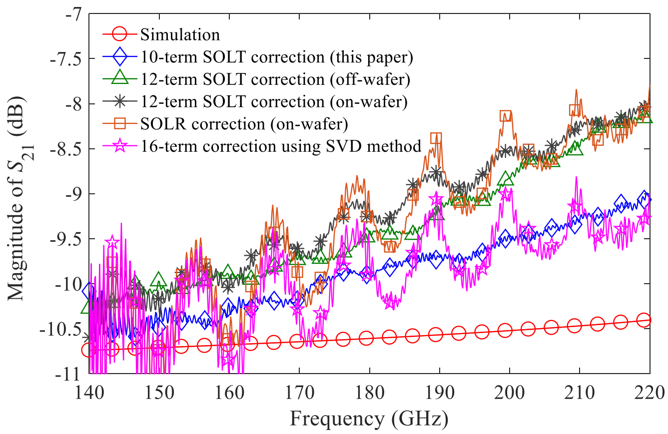

Fig. 8. Comparison of attenuator transmission coefficients measured with and without crosstalk corrections.

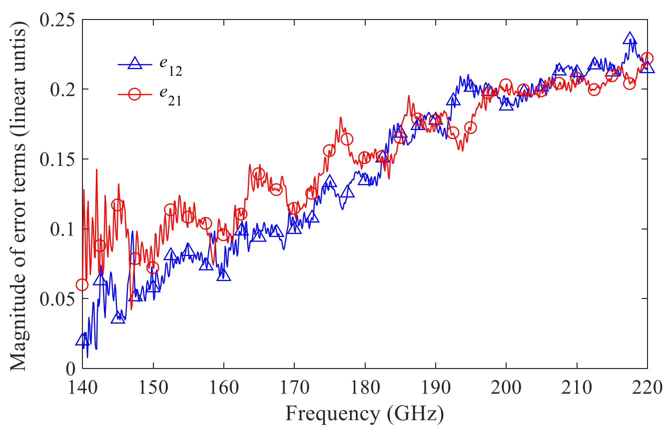

Fig. 9. Magnitude of e_{12} and e_{21} terms. To some extent, these error terms represent crosstalk between probes.

method using standards on a GGB's CS-15 calibration wafer (i.e., the off-wafer results). We also compared the results with other commonly used on-wafer calibration methods, i.e., the SOLR method, and the 16-term correction using the SVD method [6], [13], with only four standards (i.e., a short–short pair, an open–open pair, a load–load pair, and a thru standard) from the GaAs substrate. It is clear that the magnitude corrected by 16-term correction and our method are significantly closer to the simulation results, compared to either the "on-wafer" 12-term SOLT method, the "off-wafer" 12-term SOLT method, or the SOLR method. The main reason for this is that these calibration techniques do not correct for the effect of crosstalk properly; therefore, the crosstalk contributes to the total power transmission between the probes. Besides, from Fig. 8, we can also see that there are fewer ripples in the trace using 10-term SOLT correction compared with that using 16-term correction. The main reason for this is that there is not enough information for the 16-term error model even though the SVD algorithm is applied for eliminating singular solutions. The 10-term error, reported in this paper, can effectively avoid singular solutions, as well as using only four standards.

In addition, for the "off-wafer calibration," the probe launch difference between the calibration substrate and the DUT also makes a difference because pad parasitic effects will cause additional measurement error. On the other hand, for the "on-wafer calibration," the standards are fabricated on the same wafer as the DUT. The standards are created with the identical launch as the DUT, with the same metal pad pattern and substrate dielectric.

Fig. 9 shows the derived probe-to-probe crosstalk, in linear units, using the 10-term error model. The two error terms e_{21} and e_{12} represent the forward and reverse leakage paths between the probes. One can see that the crosstalk term increases as a function of frequency and reaches 0.2 at around 200 GHz. This amount of error could cause a significant effect on a device measurement of gain or insertion loss, if not properly corrected.

IV. Conclusion

We have presented a new SOLT calibration method using a 10-term error model which is different from the conventional SOLT method in which a 12-term error model is used. The proposed 10-term error model is a simplified version of the 16-term error model that only takes into account the probe-to-probe crosstalk. Experimental results have shown this assumption to be acceptable. With this assumption, the number of error terms in the 16-term error model is reduced, and therefore, a complete solution without singularities can be derived using four sets of two-port standards. The implementation of the calibration method was carried out on a G-band on-wafer system and tested using a 10-dB attenuator. The results show that the new calibration method is much better than the conventional SOLT method by achieving an almost 1 dB (i.e., 10%) improvement in measurement accuracy. In addition, one can also see that the magnitude of the crosstalk coefficients, or error terms, increases as the frequency increases and can play a significant role in the actual device measurement.

This paper has only discussed the correction of probe coupling when the crosstalk is assumed constant. In fact, the probe coupling may also contain some multimodal signals which are more difficult to characterize. However, the experimental results in this paper have shown that the crosstalk correction technique described in this paper has produced substantial improvement to on-wafer S-parameter measurements. In the future, we intend to extend this work to take account of any effects that may be present due to multimode probe coupling.

Acknowledgment

The authors would like to thank the Hebei Semiconductor Research Institute, Shijiazhuang, China, for fabricating the samples and Dr. J. Wang, University of Glasgow, Glasgow, U.K., for taking the SEM image of the attenuator.

References

[1] J. Fitzpatrick, "Error models for systems measurement," *Microw. J.*, vol. 21, no. 5, pp. 63–66, May 1978.
[2] D. Rytting, "An analysis of vector measurement accuracy enhancement techniques," in *Proc. RF Microw. Symp. Exhib.*, 1980.

[3] G. F. Engen and C. A. Hoer, "Thru-reflect-line: An improved technique for calibrating the dual six-port automatic network analyzer," *IEEE Trans. Microw. Theory Techn.*, vol. MTT-27, no. 12, pp. 987–993, Dec. 1979.

[4] A. Davidson, K. Jones, and E. Strid, "LRM and LRRM calibrations with automatic determination of load inductance," in *36th ARFTG Conf. Dig.-Fall*, Monterey, CA, USA, Nov. 1990, pp. 57–63.

[5] R. A. Speciale, "A generalization of the TSD network-analyzer calibration procedure, covering n-port scattering-parameter measurements, affected by leakage errors," *IEEE Trans. Microw. Theory Techn.*, vol. MTT-25, no. 12, pp. 1100–1115, Dec. 1977.

[6] J. V. Butler, D. K. Rytting, M. F. Iskander, R. D. Pollard, and M. V. Bossche, "16-term error model and calibration procedure for on-wafer network analysis measurements," *IEEE Trans. Microw. Theory Techn.*, vol. 39, no. 12, pp. 2211–2217, Dec. 1991.

[7] H. Heuermann and B. Schiek, "Calibration of network analyser measurements with leakage errors," *Electron. Lett.*, vol. 30, no. 1, pp. 52–53, Jan. 1994.

[8] K. Silvonen, K. Dahlberg, and T. Kiuru, "16-term error model in reciprocal systems," *IEEE Trans. Microw. Theory Techn.*, vol. 60, no. 11, pp. 3551–3558, Nov. 2012.

[9] K. Dahlberg and K. Silvonen, "A method to determine LRRM calibration standards in measurement configurations affected by leakage," *IEEE Trans. Microw. Theory Techn.*, vol. 62, no. 9, pp. 2132–2139, Sep. 2014.

[10] M. Schramm, M. Hrobak, J. Schür, and L.-P. Schmidt, "A SOLR calibration procedure for the 16-term error model," in *Proc. 42nd Eur. Microw. Conf.*, Amsterdam, The Netherlands, Oct./Nov. 2012, pp. 589–592.

[11] D. F. Williams, F.-J. Schmückle, R. Doerner, G. N. Phung, U. Arz, and W. Heinrich, "Crosstalk corrections for coplanar-waveguide scattering-parameter calibrations," *IEEE Trans. Microw. Theory Techn.*, vol. 62, no. 8, pp. 1748–1761, Aug. 2014.

[12] K. J. Silvonen, "Calibration of 16-term error model (microwave measurement)," *Electron. Lett.*, vol. 29, no. 17, pp. 1544–1545, Aug. 1993.

[13] X. Wei, G. Niu, S. L. Sweeney, and S. S. Taylor, "Singular-value-decomposition based four port de-embedding and single-step error calibration for on-chip measurement," in *IEEE MTT-S Int. Microw. Symp. Dig.*, Honolulu, HI, USA, Jun. 2007, pp. 1497–1500.

[14] K. Silvonen, "LMR 16—A self-calibration procedure for a leaky network analyzer," *IEEE Trans. Microw. Theory Techn.*, vol. 45, no. 7, pp. 1041–1049, Jul. 1997.

[15] K. J. Silvonen, "A general approach to network analyzer calibration," *IEEE Trans. Microw. Theory Techn.*, vol. 40, no. 4, pp. 754–759, Apr. 1992.

[16] K. Silvonen, "New five-standard calibration procedures for network analyzers and wafer probes," Circuit Theory Lab., Helsinki Univ. Technol., Espoo, Finland, Tech. Rep. CT-19, Mar. 1994. [Online]. Available: http://www.aplac.hut.fi

[17] N. M. Ridler and R. G. Clarke, "Establishing traceability to the international system of units for scattering parameter measurements from 750 GHz to 1.1 THz," *IEEE Trans. THz Sci. Technol.*, vol. 6, no. 1, pp. 2–11, Jan. 2016.

[18] V. Teppati and A. Ferrero, "A comparison of uncertainty evaluation methods for on-wafer S-parameter measurements," *IEEE Trans. Instrum. Meas.*, vol. 63, no. 4, pp. 935–942, Apr. 2014.

[19] K. Jones and E. Strid, "Where are my on-wafer reference planes?" in *30th ARFTG Conf. Dig.–Winter*, Dallas, TX, USA, Dec. 1987, pp. 27–40.

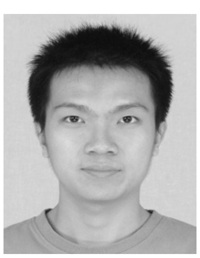

Chen Liu was born in Hengshui, Hebei, China, in 1986. He received the B.E. and M.E. degrees in measuring and testing technologies and instruments from Xidian University, Xi'an, China, in 2009 and 2012, respectively.

He joined the Metrology Centre, Hebei Semiconductor Research Institute, Shijiazhuang, China, as a Research Engineer in 2012. In 2017, he joined the National Physical Laboratory, Teddington, U.K., as a Visiting Researcher. His current research interests include the design and characterizing of on-wafer SOLT and TRL S-parameters calibration kits, the development of accurate on-wafer S-parameters and noise parameter measurement techniques, and the verification of on-wafer S-parameters and noise parameter using active and passive devices.

Aihua Wu was born in Zhangjiakou, China, in 1980. He received the B.S. and M.E. degrees in microelectronics from Jilin University, Changchun, China, in 2004 and 2007, respectively.

He joined the Hebei Semiconductor Research Institute, Shijiazhuang, in 2007, where he is currently a Senior Research Engineer with the Metrology Centre. In 2017, he joined the National Physical Laboratory, Teddington, U.K., as a Visiting Researcher. His current research interests include microwave metrology, particularly on-wafer noise measurements and instrumentation, and the fabrication of on-wafer devices for ultra-wideband S-parameters and noise parameter calibration and verification.

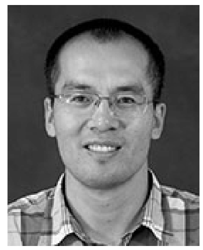

Chong Li (M'12–SM'17) was born in Liaoning, China, in 1979. He received the B.Eng. degree from Donghua University, Shanghai, China, in 2002, the M.Sc. degree (Distinction) from The University of Manchester, Manchester, U.K., in 2007, and the Ph.D. degree in electronics and electrical engineering from the University of Glasgow, Glasgow, U.K., in 2011.

He joined the University of Glasgow as a Post-Doctoral Research Assistant in 2011, and then became a Post-Doctoral Research Associate, where he was involved in the development of millimeter-wave signal sources and terahertz imaging systems. In 2014, he joined the National Physical Laboratory (NPL), Teddington, U.K., as a Higher Research Scientist, where he contributed and led several commercial projects and U.K. national and European research projects. He was the Measurement Service Provider of the ultrafast waveform metrology service with NPL. He also led microwave and millimeter-wave on-wafer measurements. He held a visiting position with the Advanced Technology Institute, University of Surrey, Guildford, U.K., in 2017. He joined the University of Glasgow, as a Lecturer in 2017. He has authored or co-authored more than 50 journal and conference papers. His current research interests include microwave and terahertz components, systems and metrology, and next-generation wireless communications.

Dr. Li was a recipient of the Best Non-Student Paper Prize of the Loughborough Antennas and Propagation Conference in 2015. He is an Associate Editor of *Royal Society Open Science.*

Nick Ridler (M'03–SM'06–F'14) received the B.Sc. degree from King's College, University of London, London, U.K., in 1981.

He has more than 35 years' working experience with industrial, government, and academic research establishments. He is currently the Science Leader for electromagnetics and a Principal Research Scientist with the National Physical Laboratory, Teddington, U.K. He is a Fellow of Nonlinear Microwave Measurement, Advanced Technology Institute, University of Surrey, Guildford, U.K. He is also a Non-Executive Director with LA Techniques Ltd., Surbiton, U.K., and a Visiting Professor with the Institute of Microwaves and Photonics, The University of Leeds, Leeds, U.K., Department of Electrical Engineering and Electronics, University of Liverpool, Liverpool, U.K., and Advanced Technology Institute, University of Surrey. His current research interests include high-frequency precision electromagnetic measurement (1 kHz–1 THz).

Mr. Ridler is a Fellow of the Institution of Engineering and Technology and the Institute of Physics. He is currently the Chair of the IEEE MTT-S's Standards Coordinating Committee. He was the Chair of the IEEE MTT-S's Microwave Measurements Technical Committee and the President of the Automatic RF Techniques Group.